ISSN 1453 – 7303 "HIDRAULICA" (No. 4/2019)
Magazine *of Hydraulics, Pneumatics, Tribology, Ecology, Sensorics, Mechatronics*

The Influence of Corrosion and Temperature Variation on a CNG Storage Tank with a Combined Form consisting of a Torus and a Sphere

Assoc. Prof. PhD. Eng. **Mihai ŢĂLU**[1], Assoc. Prof. PhD. Eng. **Ștefan ŢĂLU**[2,*]

[1] University of Craiova, Faculty of Mechanics, Department of Applied Mechanics and Civil Engineering, Calea București Street, no. 107, 200512 Craiova, Dolj county, Romania. E-mail: mihai_talu@yahoo.com

[2] Technical University of Cluj-Napoca, The Directorate of Research, Development and Innovation Management (DMCDI), Constantin Daicoviciu Street, no. 15, Cluj-Napoca, 400020, Cluj county, Romania. Corresponding author* e-mail: stefan_ta@yahoo.com

Abstract: *The objective of this paper is to study the influence of corrosion and temperature variation on a CNG storage tank with a combined form consisting of a torus and a sphere, made of steel, for compressed natural gas (CNG) storage from the automotive industry. Numerical simulations had been performed to assess the influence of the corrosion and temperature variation on the state of stress and of the linear deformation values. A polynomial interpolation was applied to provide a comparison between the surfaces or curves.The 3-D (three-dimensional) model (modelled using the AutoCAD Autodesk 2017 software), was imported for numerical analyses to SolidWorks 2017 software). The results of analyzed cases can improve the fundamental understanding of the corrosion behavior of CNG storage tanks in exploatation environments.*

Keywords: *Automotive industry, compressed natural gas (CNG) storage tank, industrial engineering design, optimization methods, pressure vessel*

1. Introduction

In the last few decades, the process of deterioration of materials due to the storage fuel tank's interaction with interconnected components and corrosive environmental conditions has been deeply studied in the scientific literature, both theoretically and experimentally, in relation with a lot of factors (such as erosion, the degree of saturation with water, the elastic properties and the strength of the material, the pore structure of the material, volume change of the material, the volume changes of the material in pores, dissolution of a material and the associated chemical changes) [1]. Furthermore, in the scientific literature are presented new models for the competitive market of fuel storage tanks designed based on suitable strategies for reducing the impact of corrosion, and preserving the material integrity [2-7].
Generally, the fuel storage tanks are made of materials with good mechanical and chemical resistance; they have simple or complex geometric configurations, in a wide range of dimensions, with various engineering specifications, which combines design, functionality and performance [8-12].
Modern computer aided design (CAD) and computer aided engineering (CAE) analyses used in designing of the storage fuel tanks have become a part of product development process that offer a competitive advantage, without substantial investments, for reducing product design cycle by saving time, costs in set ups and manufacturing the physical prototypes [13-16].
In the design and manufacturing strategies of the storage fuel tanks, priority research directions include optimization theory and algorithms for analysis, methodologies for multiscale deterministic models; alternative models of uncertainty and risk; integration of data and modeling [17-21].
For the 3-D (three-dimensional) design of the storage fuel tanks in accordance with the relevant guidelines and procedures outlined by the national/international standards [22-26] there are various valid implementations of mathematical methods [27-31] in more efficient algorithms and programs [32-36] to find the optimized solution according the criterion of optimality to satisfy the general structural design (In a hierarchical approach, the system, subsystems, components) [37-42] and certification rules [43, 44].
In our research, the influence of corrosion and temperature variation on a CNG storage tank with a combined form consisting of a torus and a sphere, made of steel, for compressed natural gas (CNG) storage from the automotive industry was performed in accordance to the general structural design.

2. Design methodology

2.1 Basic geometry of the parametric 3-D model

Let's consider the parametric 3-D model of a CNG storage tank composed by a torus and a sphere with eight intermediate bracelets as shown in fig. 1, as described in Ref. [18].

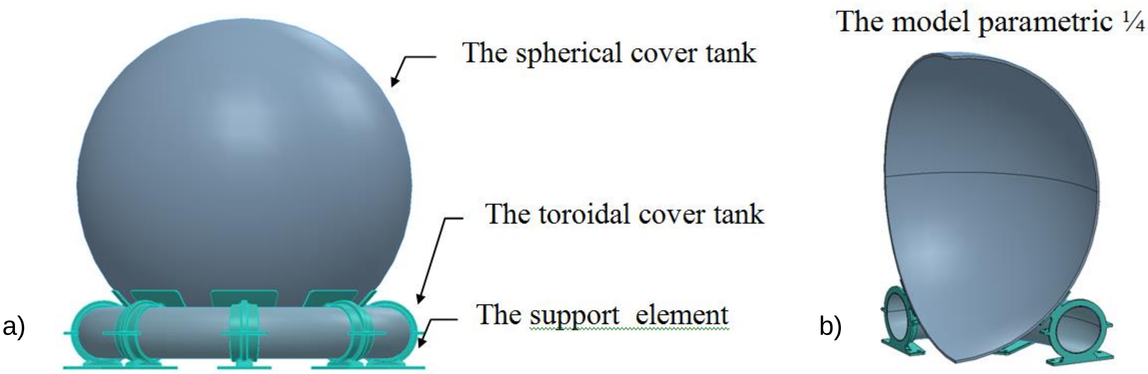

Fig. 1. The graphical representation of the parametric 3-D model of a CNG storage tank composed by a torus and a sphere with eight intermediate bracelets

2.2 Numerical analysis of the parametric 3-D model

Based on the physical model, the modeling was done in the AutoCAD Autodesk 2017 software [45] and the numerical analysis was performed with SolidWorks 2017 software [46] with the Static, Thermal and Design Study modules. The design data used were:

- the tank material is AISI 4340 steel; the intermediate bracelet type element is AISI 1045 steel;
- the maximum hydraulic test pressure: p_{max} = 300 bar;
- the working temperature between the limits: T = -30 ^{0}C up to T = 60 ^{0}C;
- the period of the tank exploitation: n_a = 20 years;
- the corrosion rate of the material: v_c = 0.06 mm/years.
- the fuel stored in the tank is CNG with a density of ρ = 20.5 kg / m^3.

The values of the state of stress Von Mises for spherical and toroidal covers determined by the finite element method are shown in tables 1 and 2.

Table 1: The Von Misess effort for the spherical cover

σ [MPa]	n_a years]	The spherical cover			
T [°C]	0	5	10	15	20
-30	650.99	655.91	665.28	669.9	672.79
-20	646.53	651.54	660.33	665.2	668.34
-10	642.09	647.19	655.41	660.52	663.9
0	637.67	642.87	650.51	655.87	659.49
10	633.28	638.57	645.23	651.25	655.1
20	628.92	634.29	640.81	646.65	650.74
30	624.58	630.04	636.42	642.09	646.41
40	620.27	625.82	632.06	637.56	642.1
50	615.99	621.63	627.72	633.06	637.83
60	611.75	617.47	623.42	628.59	633.59

Table 2: The Von Misess effort for the toroidal cover

σ [MPa]	n_a years]	The toroidal cover			
T [°C]	**0**	**5**	**10**	**15**	**20**
-30	558.44	570.27	613.23	636.09	625.65
-20	550.12	562.4	609.99	632.87	622.5
-10	542.02	544.73	606.88	629.8	619.49
0	534.14	547.3	603.92	626.9	616.63
10	526.53	540.12	606.41	624.18	613.93
20	519.22	533.24	603.89	621.67	611.41
30	512.23	526.67	601.59	619.36	609.09
40	505.61	520.44	599.52	617.27	606.98
50	499.44	514.62	597.7	615.41	605.11
60	493.7	509.02	596.11	613.79	603.48

The graphs and laws of the variance of the Von Misess effort, calculated through a polynomial interpolation using Microsoft Excel 2017, taking into account the results from table 1 and 2, are graphically shown in fig. 2.

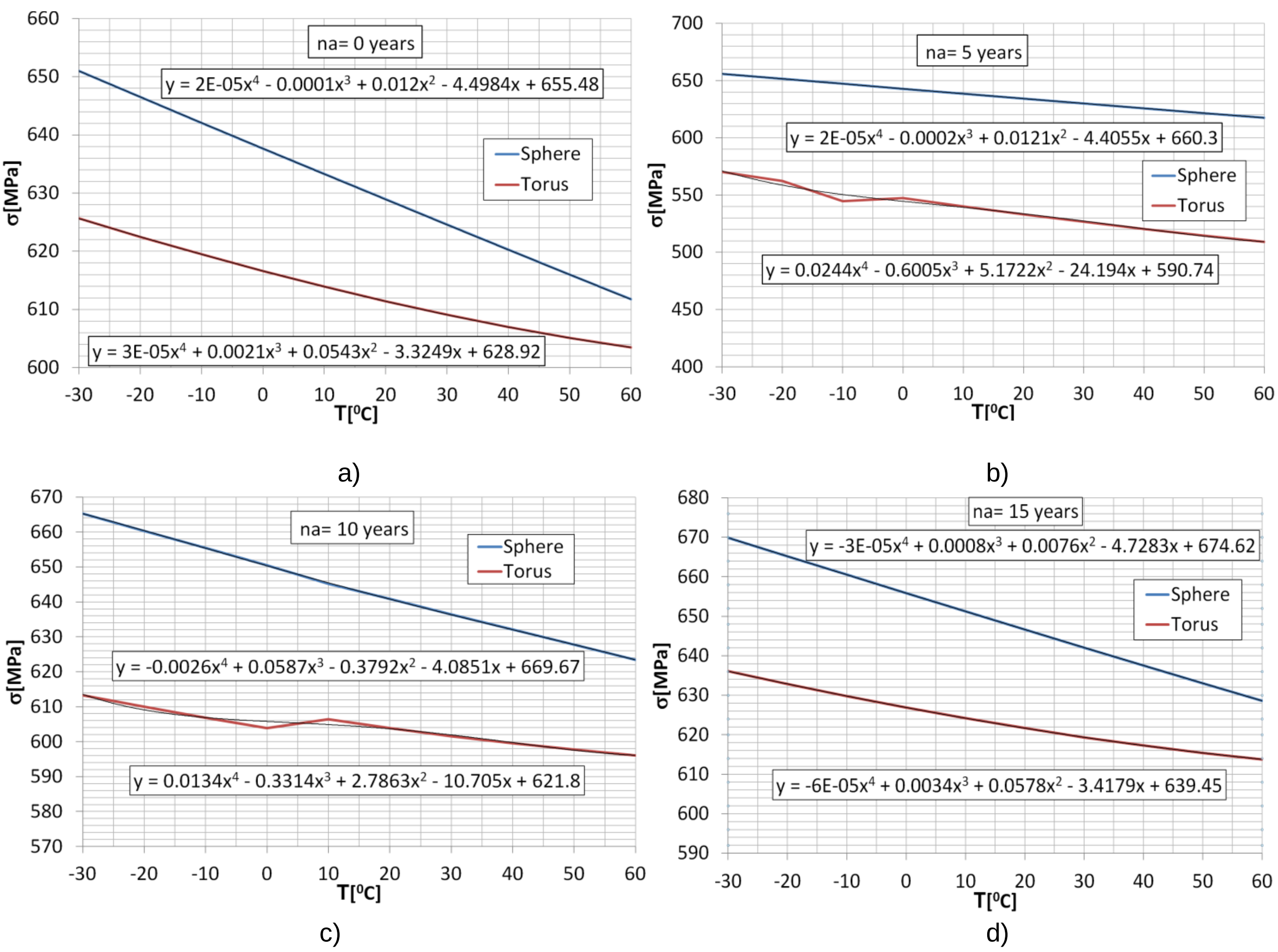

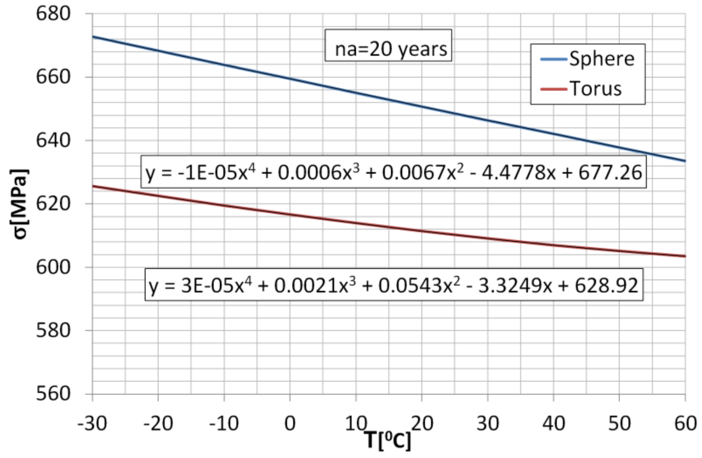

e)

Fig. 2. The graph of Von Mises stress σ = f(T) for spherical and toroidal covers

The graphs of 3-D surfaces corresponding to the Von Mises effort σ = f(T, n_a) taking into account the results from table 1 and 2, are graphically shown in fig. 3.

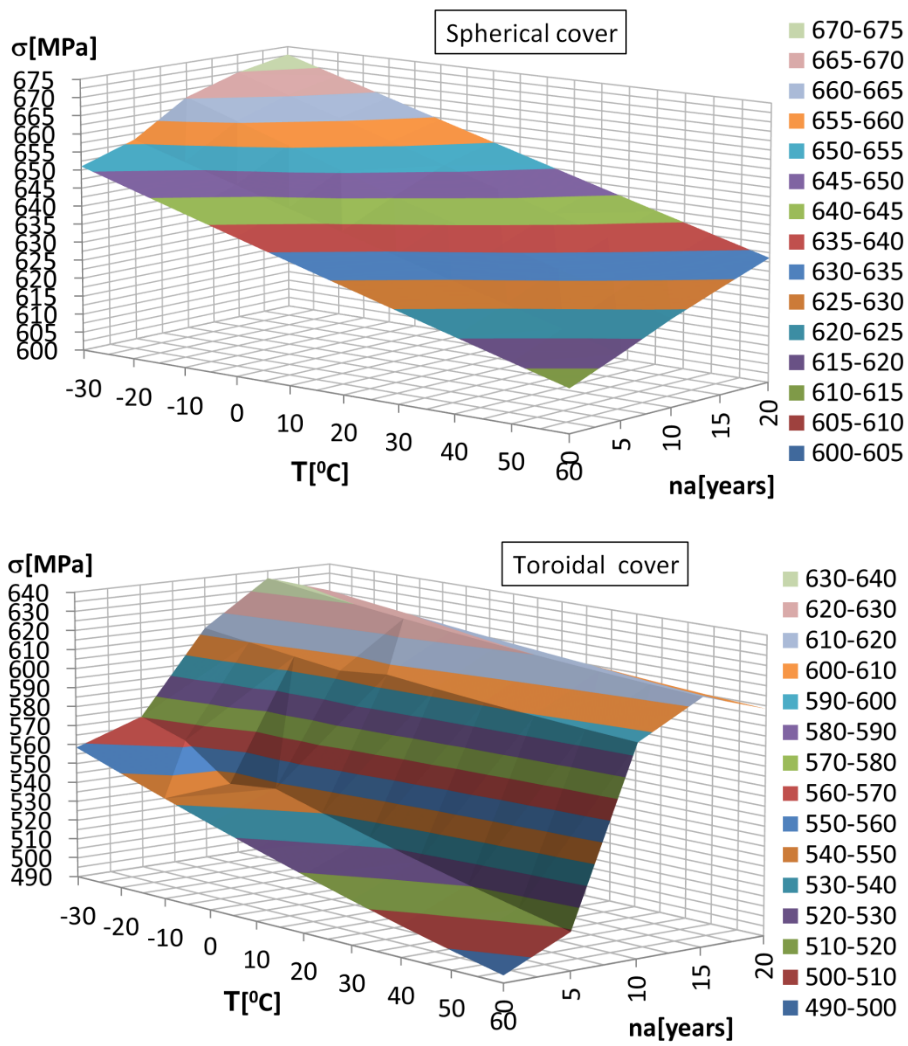

a)

b)

Fig. 3. The graphs of 3-D surfaces corresponding to the Von Mises effort σ = f(T, n_a) for: a) spherical and b) toroidal covers

The resulting value of maximum Von Mises stress occurs at a minimum temperature of T = -30 ^{0}C and a maximum linear deformation at a temperature of T = 60 ^{0}C.
Distributions of the state of Von Mises stress for the storage tank corresponding for n_a = {0, 5, 10, 15, 20} years are shown in fig. 4.

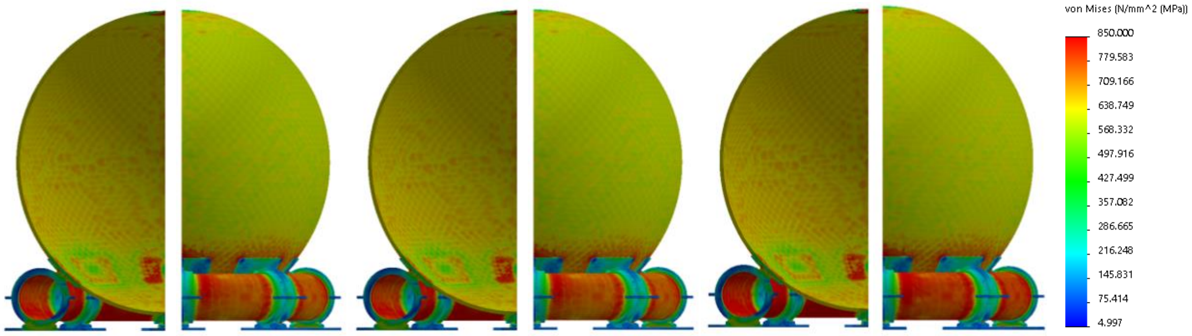

a) b) c)

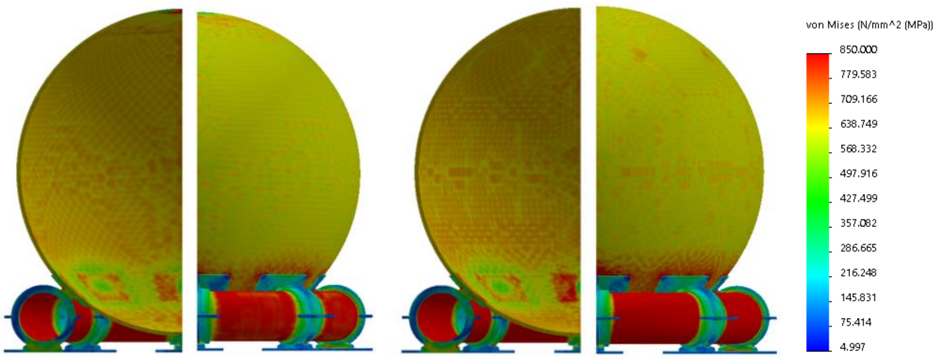

d) e)

Fig. 4. The graphs of distributions of Von Mises stress $\sigma = f(n_a)$ for the storage tank: a) n_a = 0 years; b) n_a = 5 years; c) n_a = 10 years; d) n_a = 15 years; e) n_a = 20 years

The values of the resultant linear deformation for spherical and toroidal covers determined by numerical analyses are shown in tables 3 and 4.

Table 3: The resultant liniar deformation for the spherical cover

u [mm]	**n_a years]**	**The spherical cover**			
T [°C]	**0**	**5**	**10**	**15**	**20**
-30	2.809	2.837	2.983	2.832	2.920
-20	2.879	2.907	3.056	2.899	2.997
-10	2.949	2.977	3.129	2.966	3.069
0	3.018	3.047	3.202	3.034	3.141
10	3.088	3.118	3.500	3.101	3.212
20	3.158	3.188	3.575	3.169	3.284
30	3.228	3.258	3.650	3.236	3.356
40	3.298	3.328	3.725	3.304	3.428
50	3.368	3.399	3.800	3.371	3.500
60	3.438	3.469	3.875	3.439	3.573

Table 4: The resultant liniar deformation for the toroidal cover

u [mm]	n_a [years]	The toroidal cover			
T [°C]	0	5	10	15	20
-30	1.571	1.589	1.718	1.703	1.740
-20	1.588	1.606	1.735	1.718	1.757
-10	1.606	1.624	1.751	1.733	1.774
0	1.623	1.641	1.768	1.748	1.792
10	1.641	1.659	1.955	1.763	1.809
20	1.659	1.677	1.972	1.779	1.827
30	1.677	1.694	1.990	1.795	1.845
40	1.695	1.712	2.008	1.811	1.741
50	1.713	1.731	2.026	1.827	1.881
60	1.731	1.749	2.045	1.843	1.900

The graphs and laws of the variance of the resultant linear deformation, calculated through a polynomial interpolation using Microsoft Excel 2017, taking into account the results from tables 3 and 4, are graphically shown in fig. 5.

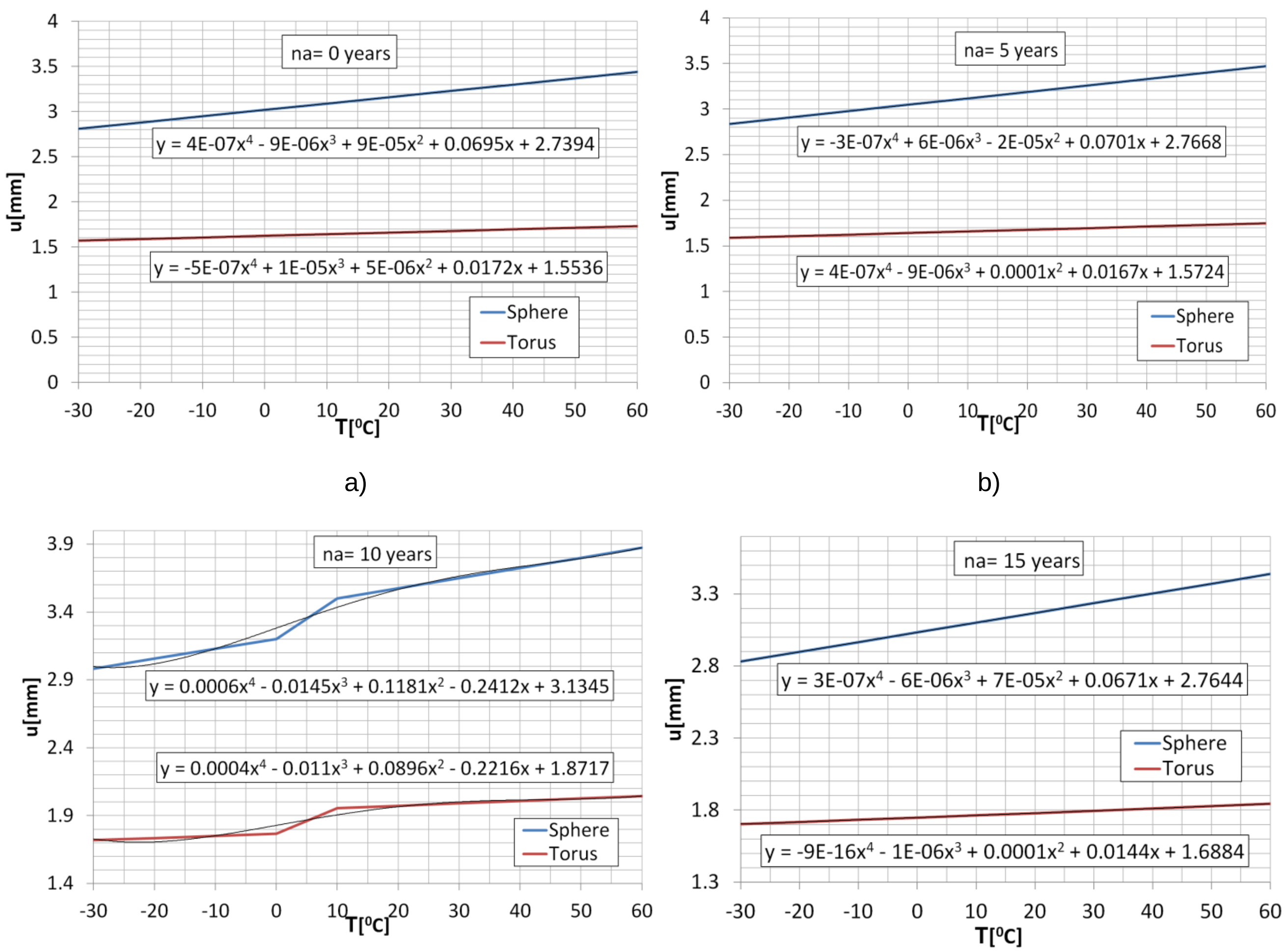

a) b)

c) d)

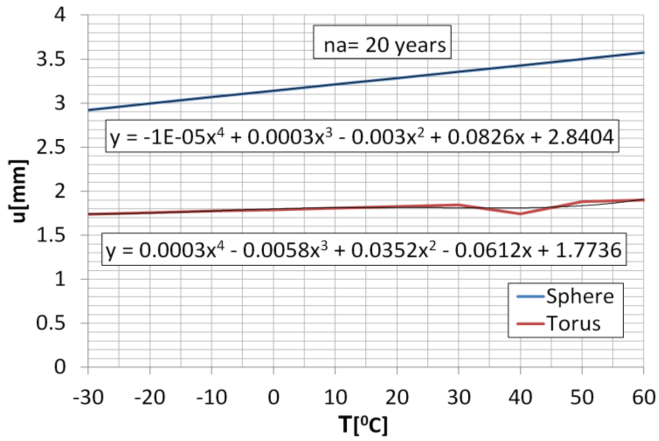

e)

Fig. 5. The graphs and laws of the variance of the resultant linear deformation u = f(T) for spherical and toroidal covers

The graphs of 3-D surfaces corresponding to the resultant linear deformation u = f(T, n_a) taking into account the results from tables 3 and 4, are graphically shown in fig. 6.

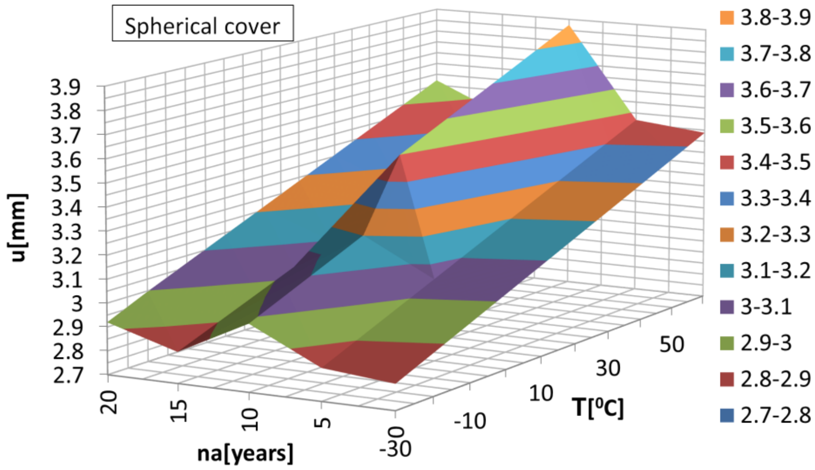

a)

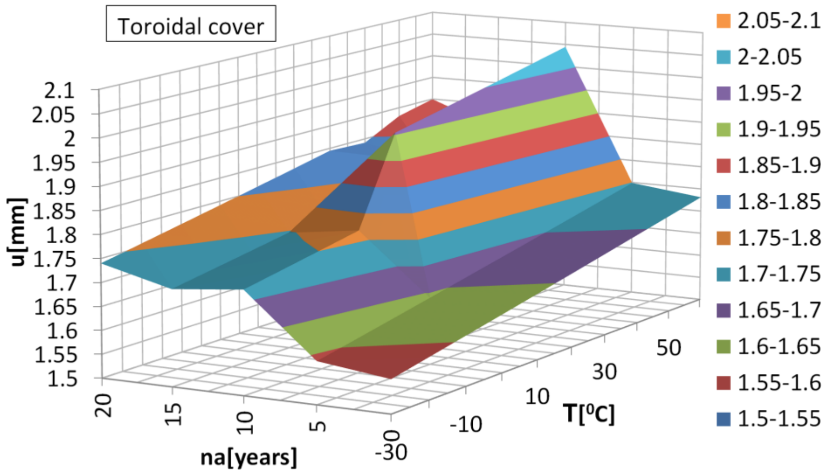

b)

Fig. 6. The graphs of 3-D surfaces corresponding to the resultant linear deformation u = f(T, n_a) for: a) spherical and b) toroidal covers

Distributions of the resultant maximum liniar deformation at a temperature of T = 60 ^{0}C for the storage tank corresponding for $n_a = \{0, 5, 10, 15, 20\}$ years are shown in fig. 7.

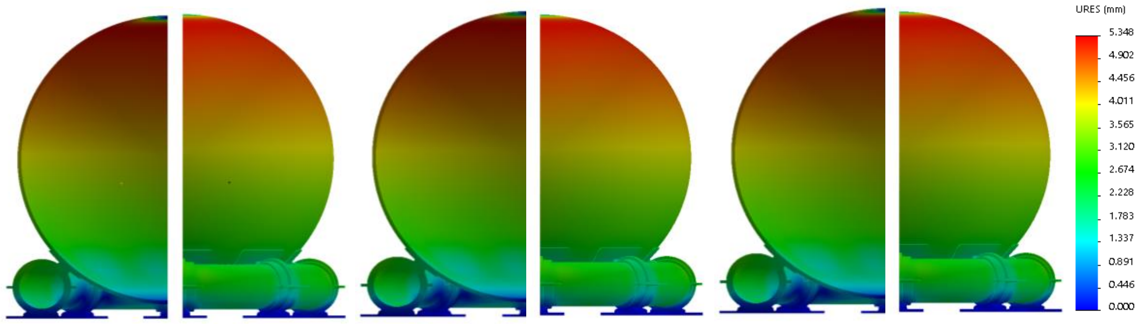

a) b) c)

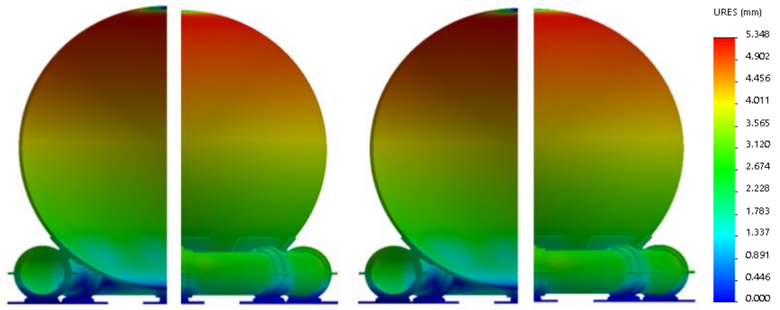

d) e)

Fig. 7. The graphs of distributions of the resultant liniar deformation at a temperature of T = 60 ^{0}C, $u = f(n_a)$ for the storage tank: a) n_a = 0 years; b) n_a = 5 years; c) n_a = 10 years; d) n_a = 15 years; e) n_a = 20 years

The parameters $\Delta\sigma = f(T, n_a)$ and $\Delta u = f(T, n_a)$ for the spherical cover are given in tables 5 and 6.

Table 5: The variation of the Von Mises effort $\Delta\sigma = f(T, n_a)$ for the spherical cover

$\Delta\sigma$ [%]	T [°C]	The spherical cover								
n_a [years]	-30	-20	-10	0	10	20	30	40	50	60
0	0.00	0.00	0.00	0.00	0.00	0.00	0.00	0.00	0.00	0.00
5	0.76	0.77	0.79	0.82	0.84	0.85	0.87	0.89	0.92	0.94
10	2.15	2.09	2.03	1.97	1.85	1.86	1.86	1.87	1.87	1.87
15	2.82	2.81	2.79	2.77	2.76	2.74	2.73	2.71	2.70	2.68
20	3.24	3.26	3.29	3.31	3.33	3.35	3.38	3.40	3.42	3.45

Table 6: The variation of the resultant liniar deformation $\Delta u = f(T, n_a)$ for the spherical cover

Δu [%]	T [°C]	The spherical cover								
n_a [years]	-30	-20	-10	0	10	20	30	40	50	60
0	0.00	0.00	0.00	0.00	0.00	0.00	0.00	0.00	0.00	0.00
5	0.76	0.99	0.98	0.97	0.95	0.95	0.93	0.92	0.92	0.91
10	2.15	5.84	5.80	5.77	5.74	11.76	11.65	11.55	11.45	11.35
15	2.82	0.79	0.69	0.59	0.50	0.41	0.33	0.24	0.16	0.09
20	3.24	3.80	3.95	3.92	3.89	3.86	3.84	3.81	3.79	3.77

The graphs of 3-D surfaces corresponding to the parameters $\Delta\sigma$ = f(T, n_a) and Δu = f(T, n_a) for the spherical cover taking into account the results from tables 5 and 6, are graphically shown in fig. 8.

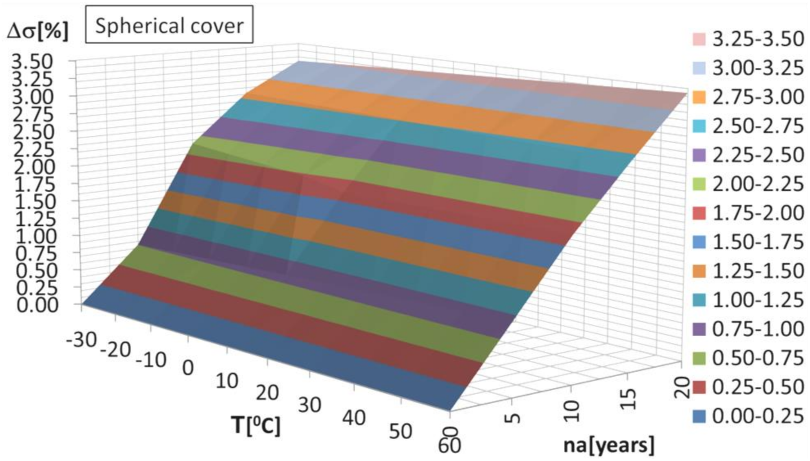

a)

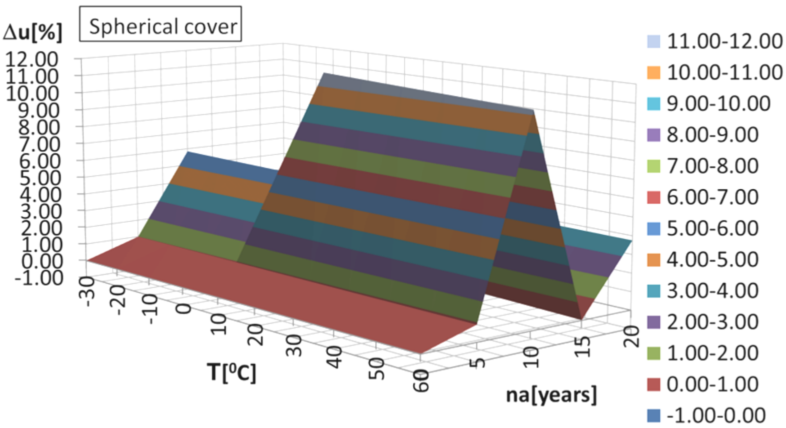

b)

Fig. 8. The graphs of 3-D surfaces corresponding for the spherical cover: a) $\Delta\sigma$ = f(T, n_a), and b) Δu = f(T, n_a)

The parameters $\Delta\sigma$ = f(T, n_a) and Δu = f(T, n_a) for the toroidal cover are given in tables 7 and 8.

Table 7: The variation of the Von Mises effort $\Delta\sigma$ = f(T, n_a) for the toroidal cover

Δσ [%]	**T [°C]**	**The toroidal cover**								
n_a [years]	**-30**	**-20**	**-10**	**0**	**10**	**20**	**30**	**40**	**50**	**60**
0	0.00	0.00	0.00	0.00	0.00	0.00	0.00	0.00	0.00	0.00
5	2.12	2.23	0.50	2.46	2.58	2.70	2.82	2.93	3.04	3.10
10	8.93	9.81	10.69	11.55	13.17	14.02	14.85	15.66	16.44	17.18
15	12.21	13.08	13.94	14.80	15.64	16.48	17.30	18.09	18.84	19.57
20	10.74	11.63	12.51	13.38	14.24	15.08	15.90	16.70	17.46	18.19

Table 8: The variation of the resultant liniar deformation Δu = f(T, n_a) for the toroidal cover

Δu [%]	**T [°C]**	**The toroidal cover**								
n_a [years]	**-30**	**-20**	**-10**	**0**	**10**	**20**	**30**	**40**	**50**	**60**
0	0.00	0.00	0.00	0.00	0.00	0.00	0.00	0.00	0.00	0.00
5	1.18	1.15	1.13	1.12	1.10	1.09	1.07	1.05	1.03	1.02
10	8.59	8.45	8.32	8.20	16.06	15.90	15.75	15.61	15.47	15.33
15	7.76	7.54	7.34	7.15	6.95	6.77	6.59	6.42	6.25	6.09
20	9.72	9.62	9.51	9.41	9.30	9.21	9.11	2.68	8.95	8.87

The graphs of 3-D surfaces corresponding to the parameters $\Delta\sigma$ = f(T, n_a) and Δu = f(T, n_a) for the toroidal cover taking into account the results from tables 7 and 8, are graphically shown in fig. 9.

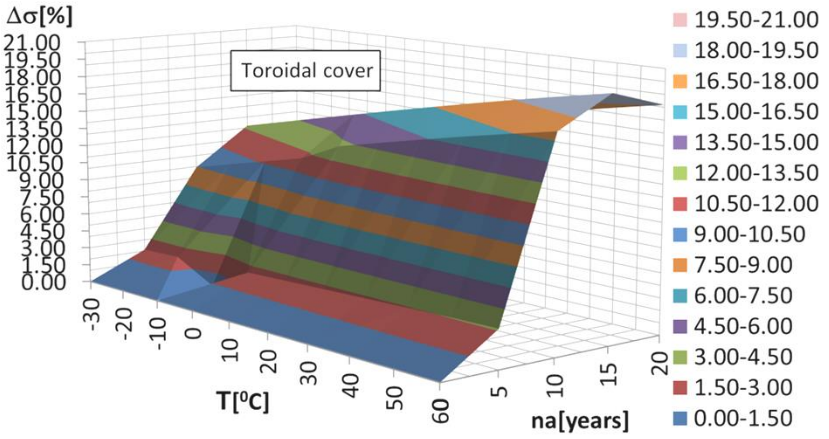

a)

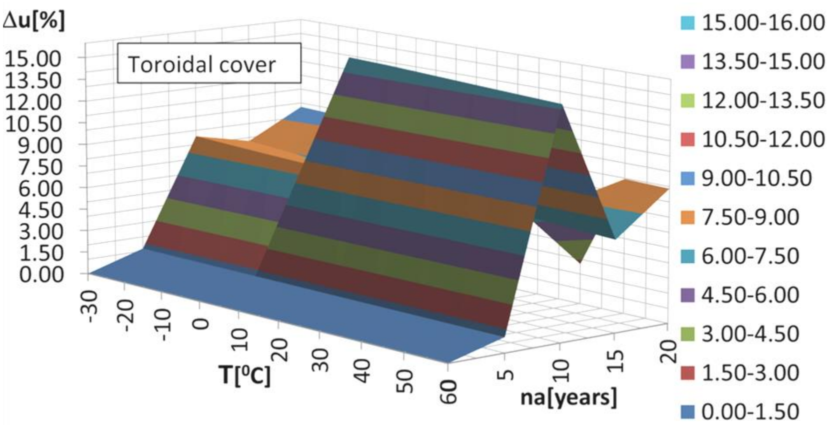

b)

Fig. 9. The graphs of 3-D surfaces corresponding for the toroidal cover: a) $\Delta\sigma$ = f(T, n_a), and b) Δu = f(T, n_a)

3. Discussion

Following the numerical analyses and the resulting graphs it has been found that:
- the evolution of corrosion over time implies the decreasing of the thickness of the tank covers, which directly determine the increasing of the Von Mises stress state (tables 1-4);
- with the decrease of the temperature, the state of effort increases and reaches a maximum value corresponding to T = -30 ^{0}C; at the same time, a decrease of the state of effort is observed with the increasing of the temperature, reaching an appropriate minimum value for T = 60 ^{0}C (fig. 2).
- the resulting linear deformation decreases at negative temperatures and increases at positive temperatures (fig. 5); also the increase of the corrosion always determines the increase of the state of deformation due to the decrease of the thickness of the walls (under a constant pressure);
- the parameter $\Delta\sigma$ increases with the increase of the n_a parameter in the tank covers (fig. 8), with higher values in the toroidal cover; also in the toroidal cover the parameter Δu increases with the increase of the n_a parameter (fig. 9).

4. Conclusions

These numerical analyses can be applied in the design phase of a CNG storage tank composed of a torus and a sphere, made of steel, used in the automotive industry.

Conflict of Interest: The authors declare that they have no conflict of interest.

ORCID: Ştefan Ţălu, http://orcid.org/0000-0003-1311-7657.

References

[1] Moncmanová, A. "Environmental factors that influence the deterioration of materials." *WIT Transactions on State of the Art in Science and Engineering* 28 (2007). DOI: 10.2495/978-1-84564-032-3/01.
[2] Ghiţă, C. Mirela, Anton C. Micu, Mihai Ţălu, Ştefan Ţălu, and Ema I. Adam. "Computer-Aided Design of a classical cylinder gas tank for the automotive industry." *Annals of Faculty of Engineering Hunedoara - International Journal of Engineering, Hunedoara*, *Romania*, Tome XI, Fascicule 4 (2013): 59-64.
[3] Ghiţă, C. Mirela, Anton C. Micu, Mihai Ţălu, and Ştefan Ţălu. "3D modelling of a shrink fitted concave ended cylindrical tank for automotive industry." *Acta Technica Corviniensis – Bulletin of Engineering, Hunedoara, Romania*, Tome VI, Fascicule 4 (2013): 87-92.
[4] Ghiţă, C. Mirela, Anton C. Micu, Mihai Ţălu, and Ştefan Ţălu. "Shape optimization of a thoroidal methane gas tank for automotive industry." *Annals of Faculty of Engineering Hunedoara - International Journal of Engineering, Hunedoara, Romania*, Tome X, Fascicule 3 (2012): 295-297.
[5] Ghiţă, C. Mirela, Anton C. Micu, Mihai Ţălu, and Ştefan Ţălu. "3D modelling of a gas tank with reversed end up covers for automotive industry." *Annals of Faculty of Engineering Hunedoara - International Journal of Engineering, Hunedoara*, *Romania*, Tome XI, Fascicule 3 (2013): 195-200.
[6] Ghiţă, C. Mirela, Anton C. Micu, Mihai Ţălu, and Ştefan Ţălu. "Shape optimization of vehicle's methane gas tank." *Annals of Faculty of Engineering Hunedoara - International Journal of Engineering, Hunedoara, Romania*, Tome X, Fascicule 3 (2012): 259-266.
[7] Ghiţă, C. Mirela, Ştefan C. Ghiță, Ştefan Ţălu, and Simona Rotaru, "Optimal design of cylindrical rings used for the shrinkage of vehicle tanks for compressed natural gas." *Annals of Faculty of Engineering Hunedoara - International Journal of Engineering, Hunedoara*, Tome XII, Fascicule 3 (2014): 243-250.
[8] Bică, Marin, Mihai Ţălu, and Ştefan Ţălu. "Optimal shapes of the cylindrical pressurized fuel tanks." *Magazine of Hydraulics, Pneumatics, Tribology, Ecology, Sensorics, Mechatronics (HIDRAULICA)*, no. 4 (December 2017): 6-17.
[9] Ţălu, Mihai. "The influence of the corrosion and temperature on the Von Mises stress in the lateral cover of a pressurized fuel tank." *Magazine of Hydraulics, Pneumatics, Tribology, Ecology, Sensorics, Mechatronics (HIDRAULICA)*, no. 4 (December 2017): 89-97.
[10] Ţălu, Mihai, and Ştefan Ţălu. "Analysis of temperature resistance of pressurized cylindrical fuel tanks." *Magazine of Hydraulics, Pneumatics, Tribology, Ecology, Sensorics, Mechatronics (HIDRAULICA)*, no. 1 (March 2018): 6-15.
[11] Vintilă, Daniela, Mihai Ţălu, and Ştefan Ţălu. "The CAD analyses of a torospheric head cover of a pressurized cylindrical fuel tank after the crash test." *Magazine of Hydraulics, Pneumatics, Tribology, Ecology, Sensorics, Mechatronics (HIDRAULICA)*, no. 4 (December 2017): 57-66.
[12] Ţălu, Ştefan, and Mihai Ţălu. "The influence of deviation from circularity on the stress of a pressurized fuel cylindrical tank." *Magazine of Hydraulics, Pneumatics, Tribology, Ecology, Sensorics, Mechatronics (HIDRAULICA)*, no. 4 (December 2017): 34-45.
[13] Ţălu, Mihai, and Ştefan Ţălu. "The influence of corrosion and temperature variation on the minimum safety factor of a 3D hexagonal toroid with regular hexagonal cross-section used in manufacturing of LPG storage tanks." *Magazine of Hydraulics, Pneumatics, Tribology, Ecology, Sensorics, Mechatronics (HIDRAULICA)*, no. 3 (August 2018): 16-25.
[14] Ţălu, Mihai, and Ştefan Ţălu. "Design and optimization of pressurized toroidal LPG fuel tanks with variable section." *Magazine of Hydraulics, Pneumatics, Tribology, Ecology, Sensorics, Mechatronics (HIDRAULICA)*, no. 1 (March 2018): 32-41.
[15] Ţălu, Ştefan, and Mihai Ţălu. "Algorithm for optimal design of pressurized toroidal LPG fuel tanks with constant section described by imposed algebraic plane curves." *Magazine of Hydraulics, Pneumatics, Tribology, Ecology, Sensorics, Mechatronics (HIDRAULICA)*, no. 2 (June 2018): 14-21.
[16] Ţălu, Mihai, and Ştefan Ţălu. "The optimal CAD design of a 3D hexagonal toroid with regular hexagonal cross-section used in manufacturing of LPG storage tanks." *Magazine of Hydraulics, Pneumatics, Tribology, Ecology, Sensorics, Mechatronics (HIDRAULICA)*, no. 2 (June 2018): 49-56.
[17] Ţălu, Ştefan, and Mihai Ţălu. "The influence of corrosion and pressure variation on the minimum safety factor of a 3D hexagonal toroid with regular hexagonal cross-section used in manufacturing of LPG storage tanks." *Magazine of Hydraulics, Pneumatics, Tribology, Ecology, Sensorics, Mechatronics (HIDRAULICA)*, no. 3 (August 2018): 39-45.
[18] Ţălu, Mihai, and Ştefan Ţălu. "Optimal design of a CNG storage tank with a combined form consisting of a torus and a sphere." *Magazine of Hydraulics, Pneumatics, Tribology, Ecology, Sensorics, Mechatronics (HIDRAULICA)*, no. 4 (December 2019): 73-82.
[19] Ţălu, Mihai, and Ştefan Ţălu. "3D geometrical solutions for toroidal LPG fuel tanks used in automotive industry." *Advances in Intelligent Systems Research* 151 (2018): 189-193. DOI: 10.2991/cmsa-18.2018.44.

[20] Ţălu, Ştefan, and Mihai Ţălu. "The Influence of corrosion on the vibration modes of a pressurized fuel tank used in automotive industry." *DEStech Transactions on Materials Science and Engineering* (May 2018): 1-6. DOI: 10.12783/dtmse/icmsa2018/20560.
[21] Ţălu, Ştefan, and Mihai Ţălu. "Constructive CAD variants of toroidal LPG fuel tanks used in automotive Industry." *Advances in Intelligent Systems Research* 159 (2018): 27-30. DOI: 10.2991/mmsa-18.2018.7.
[22] Ţălu, Mihai, and Ştefan Ţălu. "Optimal engineering design of a pressurized paralepipedic fuel tank." *Annals of Faculty of Engineering Hunedoara - International Journal of Engineering, Hunedoara, Romania*, Tome XVI, Fascicule 2 (2018): 193-200.
[23] Ţălu, Ştefan, and Mihai Ţălu. "CAD generating of 3D supershapes in different coordinate systems." *Annals of Faculty of Engineering Hunedoara - International Journal of Engineering, Hunedoara, Romania*, Tome VIII, Fascicule 3 (2010): 215-219.
[24] Niţulescu, Theodor, and Ştefan Ţălu. *Aplicaţii ale geometriei descriptive şi graficii asistate de calculator în desenul industrial / Applications of descriptive geometry and computer aided design in engineering graphics.* Cluj-Napoca, Risoprint Publishing House, 2001.
[25] Ţălu, Ştefan, and Mihai Ţălu. "A CAD study on generating of 2D supershapes in different coordinate systems." *Annals of Faculty of Engineering Hunedoara - International Journal of Engineering, Hunedoara, Romania*, Tome VIII, Fascicule 3 (2010): 201-203.
[26] Florescu-Gligore, Adrian, Ştefan Ţălu, and Dan Noveanu. *Reprezentarea şi vizualizarea formelor geometrice în desenul industrial / Representation and visualization of geometric shapes in industrial drawing.* Cluj-Napoca, U. T. Pres Publishing House, 2006.
[27] Ţălu, Ştefan, and Cristina Racocea. *Reprezentări axonometrice cu aplicaţii în tehnică / Axonometric representations with applications in technique.* Cluj-Napoca, MEGA Publishing House, 2007.
[28] Ţălu, Ştefan. *Geometrie descriptivă / Descriptive geometry.* Cluj-Napoca, Risoprint Publishing House, 2010.
[29] Racocea, Cristina, and Ştefan Ţălu. *Reprezentarea formelor geometrice tehnice în axonometrie / The axonometric representation of technical geometric shapes.* Cluj-Napoca, Napoca Star Publishing House, 2011.
[30] Ţălu, Ştefan. *Grafică tehnică asistată de calculator / Computer assisted technical graphics*. Cluj-Napoca, Victor Melenti Publishing House, 2001.
[31] Florescu-Gligore, Adrian, Magdalena Orban, and Ştefan Ţălu. *Cotarea în proiectarea constructivă şi tehnologică / Dimensioning in technological and constructive engineering graphics.* Cluj-Napoca, Lithography of The Technical University of Cluj-Napoca, 1998.
[32] Ţălu, Ştefan. *Reprezentări grafice asistate de calculator / Computer assisted graphical representations.* Cluj-Napoca, Osama Publishing House, 2001.
[33] Ţălu, Mihai. *Mecanica fluidelor. Curgeri laminare monodimensionale / Fluid mechanics. The monodimensional laminar flow.* Craiova, Universitaria Publishing House, 2016.
[34] Țălu, Mihai. *Calculul pierderilor de presiune distribuite în conducte hidraulice / Calculation of distributed pressure loss in hydraulic pipelines.* Craiova, Universitaria Publishing House, 2016.
[35] Țălu, Mihai. *Pierderi de presiune hidraulică în conducte tehnice cu secțiune inelară. Calcul numeric și analiză C.F.D. / Hydraulic pressure loss in technical piping with annular section. Numerical calculation and C.F.D.* Craiova, Universitaria Publishing House, 2016.
[36] Ţălu, Ştefan. *Limbajul de programare AutoLISP. Teorie şi aplicaţii / AutoLISP programming language. Theory and applications*. Cluj-Napoca, Risoprint Publishing House, 2001.
[37] Ţălu, Ştefan, and Mihai Ţălu. *AutoCAD 2006. Proiectare tridimensională / AutoCAD 2006. Three-dimensional designing*. Cluj-Napoca, MEGA Publishing House, 2007.
[38] Ţălu, Ştefan. *AutoCAD 2005*. Cluj-Napoca, Risoprint Publishing House, 2005.
[39] Ţălu, Ştefan. *AutoCAD 2017*. Cluj-Napoca, Napoca Star Publishing House, 2017.
[40] Bîrleanu, Corina, and Ştefan Ţălu. *Organe de maşini. Proiectare şi reprezentare grafică asistată de calculator / Machine elements. Designing and computer assisted graphical representations*. Cluj-Napoca, Victor Melenti Publishing House, 2001.
[41] Nedelcu, Dorian. *Proiectare și simulare numerică cu SolidWorks* / *Digital Prototyping and Numerical Simulation with SolidWorks*. Timişoara, Eurostampa Publishing House, 2011.
[42] Ţălu, Ştefan. *Micro and nanoscale characterization of three dimensional surfaces. Basics and applications*. Napoca Star Publishing House, Cluj-Napoca, Romania, 2015.
[43] *** Certification tests of LPG and CNG. Accessed August 23, 2018. http://vzlutest.cz/en/certification-tests-of-lpg-and-cng-c3.html.
[44] *** TANK software (https://cas.hexagonppm.com/solutions/tank).
[45] *** Autodesk AutoCAD 2017 software.
[46] *** SolidWorks 2017 software.